Ruthenium and Osmium Acyl Fluoride Complexes. Crystal Structure of [*OC*-6-13][RuF$_2$(CO)$_2$(PPh$_3$)$_2$]·CD$_2$Cl$_2$‡

Stuart A. Brewer, Karl S. Coleman, John Fawcett, John H. Holloway, Eric G. Hope,* David R. Russell and Paul G. Watson*,†
Department of Chemistry, University of Leicester, Leicester LE1 7RH, UK

Fluoroacyl complexes of ruthenium and osmium have been identified in the oxidative addition of XeF$_2$ to [M(CO)$_3$(PPh$_3$)$_2$] (M = Ru or Os) in dichloromethane. The mechanism of reaction, probed by the addition of BF$_3$, involves oxidation of the metal centre by XeF$^+$ followed by nucleophilic attack by F$^-$ at co-ordinated CO. For M = Ru, the fluoroacyl complex is unstable at room temperature and decomposes *via* elimination of CO to [*OC*-6-13][RuF$_2$(CO)$_2$(PPh$_3$)$_2$] for which the ligand arrangement has been confirmed by X-ray crystallography. For M = Os, the analogous complex is obtained by heating the fluoroacyl species in solution for several hours. All the products have been characterised by IR, ^{19}F and ^{31}P NMR spectroscopies.

The oxidative fluorination of five-co-ordinate iridium(I) complexes, [Ir(CO)$_3$L$_2$]$^+$ (L = PMe$_3$, PEt$_3$, PMe$_2$Ph, PEt$_2$Ph or PEtPh$_2$) with XeF$_2$ gives not only examples of rare low-valent transition-metal fluorides, but also the only examples of metal-bound fluoroacyls.[1,2] We have been investigating the reactions of XeF$_2$ with a range of ruthenium(0) and osmium(0) complexes[3,4] and report here the stepwise fluorination of neutral five-co-ordinate [M(CO)$_3$(PPh$_3$)$_2$] (M = Ru or Os), *via* the metal fluoroacyl complexes to low-valent metal fluorides.

Experimental

Proton, ^{19}F and ^{31}P NMR spectroscopic analyses were carried out on a Bruker AM300 spectrometer at 300.14, 282.41 and 75.47 MHz respectively and referenced to external SiMe$_4$, CFCl$_3$ and 85% H$_3$PO$_4$ using the high-frequency positive convention. Spectra were recorded on samples either sealed in FEP (perfluoroethylene–propylene copolymer) NMR tubes (outside diameter 4 mm) held coaxially in 5 mm precision glass NMR tubes or samples in glass NMR tubes (outside diameter 5 mm) closed with a Young's valve. Initial ^{19}F NMR spectra were recorded for *ca.* 400 scans between δ +200 and −600 using 125 000 Hz windows (*ca.* 7 Hz per point), acquisition times of 0.5 s without relaxation delays and pulse widths of 3 μs (28°). Higher-resolution spectra were recorded for narrower spectral widths dependent upon the experiment; typical data-point resolutions for 4000 scan acquisitions were *ca.* 1 Hz. Fourier transforms were carried out without exponential smoothing. The ^{31}P-{^{1}H} spectra were recorded for *ca.* 1000 scans between δ +40 and −40 using 10 000 Hz windows (*ca.* 0.5 Hz per point), acquisition times of 1.5 s with 1 s relaxation delay, pulse widths of 6 μs (30°) and composite pulse decoupling. Fourier transformations were carried out with Lorentzian line broadening of 1 Hz. Infrared spectra were recorded for Nujol mulls between KBr discs on a Diglab FTS40 FTIR spectrometer, FAB mass spectra on a Kratos Concept 1H instrument.

All preparative manipulations were carried out on a metal vacuum line with facilities to connect Teflon and FEP reaction vessels. Xenon difluoride was prepared by the static fluorination of xenon gas under UV irradiation at room temperature.[5] Tricarbonylbis(triphenylphosphine)-ruthenium[6] and -osmium[7] were prepared according to the literature methods. In typical preparations, weighed samples of [M(CO)$_3$(PPh$_3$)$_2$] (M = Ru, 0.05 g, 71 μmol; M = Os, 0.05 g, 63 μmol) and a *ca.* 10% excess of XeF$_2$ (M = Ru, 0.013 g, 78 μmol; M = Os, 0.012 g, 69 μmol) were loaded in a dry-box (< 10 ppm H$_2$O), into prefluorinated FEP reactors (outside diameter 4 mm, wall thickness 0.5 mm) fitted with polytetrafluoroethylene (ptfe) valves (Production Techniques Ltd.). After evacuation, dry CD$_2$Cl$_2$ (*ca.* 0.3 cm^3) was condensed into the reaction tube at −196 °C and the tube sealed as described previously.[8] The reaction mixture was allowed to warm slowly in the probe of the NMR spectrometer and the reaction monitored at regular temperature intervals (see below). After the NMR studies had been completed, the reaction tube was refrozen at −78 °C in an argon-filled bucket, cut open with a blade and reconnected to the vacuum line *via* a ptfe valve. The solvent was then removed under vacuum and the resulting solids transferred to the dry-box for IR spectroscopy, further reactions and NMR studies.

Crystallography.—Crystals of [*OC*-6-13][RuF$_2$(CO)$_2$(PPh$_3$)$_2$]·CD$_2$Cl$_2$, suitable for single-crystal X-ray structure determination, were obtained from a CD$_2$Cl$_2$ solution by slow vapour diffusion with diethyl ether. Crystals were isolated in a nitrogen-filled glove-bag and sealed in thin-walled glass capillaries.

Crystal data. C$_{38}$H$_{30}$F$_2$O$_2$P$_2$Ru·CD$_2$Cl$_2$, M = 806.63, monoclinic, space group $C2/c$, a = 17.075(4), b = 10.714(3), c = 19.952(5) Å, β = 102.9(1)°, U = 3558(2) Å^3 (by least-squares refinement on diffractometer angles for 31 automatically centred reflections), Z = 4, D_c = 1.66 g cm^{-3}, $F(000)$ = 1632, T = 293 K. Orange plate, crystal dimensions 0.53 × 0.48 × 0.20 mm, μ(Mo-Kα) = 0.73 mm^{-1}.

Data collection and processing. Siemens P4 diffractometer, ω mode, ω scan speed 3.0–30.0° min^{-1}, graphite-monochromated Mo-Kα radiation; 3260 reflections measured ($2 \leqslant \theta \leqslant 27°$; $-1 \leqslant h \leqslant 20$, $-1 \leqslant k \leqslant 12$, $-23 \leqslant l \leqslant 23$), 2687 unique [merging R = 0.02 after an empirical absorption correction (maximum, minimum transmission factors = 0.931, 0.781)], giving 2017 with $I > 2\sigma(I)$. No crystal decay was detected (< 2%) from periodically measured check reflections; the data were corrected for Lorentz and polarisation effects.

Structure analysis and refinement. The structure was solved by Patterson methods and refined by full-matrix least squares using the program package SHELXTL-PC.[9] The hydrogen

---

† *Present address:* Institut für Anorganische Chemie der Universität Bremen, FB2 Leobenerstrasse NW2, 28334 Bremen, Germany.

‡ *Supplementary data available:* see Instructions for Authors, *J. Chem. Soc., Dalton Trans.*, 1995, Issue 1, pp. xxv–xxx.

atoms of the phenyl groups were included in calculated positions (C–H 0.95 Å) with one overall fixed U_{iso} (= 0.08 Å^2). All non-hydrogen atoms were refined with anisotropic displacement parameters. The weighting scheme $w = 1/[\sigma^2(F_o) + 0.0045F_o^2]$, with $\sigma(F_o)$ from counting statistics, gave satisfactory agreement analyses. Final R and R' values were 0.0495 and 0.0752. The atomic coordinates for the structure are given in Table 2 and selected bond lengths and angles in Table 3.

Additional material available from the Cambridge Crystallographic Data Centre comprises H-atom coordinates, thermal parameters and remaining bond lengths and angles.

Results and Discussion

The reaction of $[Os(CO)_3(PPh_3)_2]$ with XeF_2 in dichloromethane was monitored by ^{19}F NMR spectroscopy. At 220 K two major ^{19}F NMR resonances were observed at δ 146 (F_A) and −370 (F_B) in a 1 : 1 ratio, and two minor resonances at δ −321 (F_C) and −421 (F_D). Resonance F_A is typical of a metal-bound fluoroacyl,[1,2] while those resonances with frequencies lower than δ −300 are typical of fluorine bound to osmium(II).[4] On warming the two minor resonances disappear whilst the two major resonances broaden, becoming indistinguishable from the baseline at room temperature. On cooling, these sharpen implying a reversible fluxional process. Unfortunately, it proved impossible to investigate the nature of this fluxional process because further reaction of the species occurs above room temperature (see below). At low temperatures, under high resolution, F_B exhibited triplet structure characteristic of *cis*-$^2J_{PF}$ (30 Hz).[1,2,10] The chemical shift for F_B is typical of fluoride *trans* to CO on osmium(II). The ^{31}P-{^1H} NMR spectrum at this temperature revealed a related doublet at δ 0.1 ($^2J_{PF}$ = 30 Hz) indicating a single metal-bound fluorine and confirming the synthesis of **1a**. The failure to observe the coupling between F_A and the two phosphorus atoms is not surprising since the magnitude of comparable couplings for the related iridium complexes is only a few Hz.

Removal of the solvent from the reaction mixture at this stage gave a yellow solid. The IR spectrum of this material revealed two terminal ν(CO) bands at 2053 and 1972 cm^{-1} and the ν(CO) band for the metal-bound fluoroacyl at 1651 cm^{-1}, all of which are consistent with the formulation for **1a**.

Complex **1a** appears to be fairly stable in solution at room temperature, the resonances assigned to it being still evident after standing for 2 d. However, a new ^{19}F NMR resonance at δ −305 (F_C) eventually appeared in the spectrum and grew slowly in intensity over this period. Furthermore, during attempts to investigate the fluxional process highlighted above, at elevated temperature (up to that of refluxing CD_2Cl_2), this new resonance was also observed and on recooling to 220 K was still present while the resonances assigned to **1a** had both decreased in intensity. On reflux for several hours all the resonances due to **1a** disappeared and the only one present at both 220 and 293 K was the peak at δ −305. Under high resolution this exhibited mutual triplet coupling to a related triplet at δ 1.4 ($^2J_{PF}$ = 29 Hz) in the ^{31}P-{^1H} NMR spectrum, which allowed characterisation of this second product as [*OC*-6-13][$OsF_2(CO)_2(PPh_3)_2$] **2a**, arising by elimination of CO from **1a**. Removal of the solvent from the solution now gave a buff solid. In the FAB mass spectrum the parent ion was not observed, but a series of patterns centred around *m/z* 791, 772 and 763 are readily assigned to the $[M - F]^+$, $[M - 2F]^+$ and $[M - F - CO]^+$ ions respectively. The IR spectrum of this material gave two terminal ν(CO) bands at 2017 and 1937 cm^{-1} consistent with the *cis*-octahedral formulation for **2a**.

The two minor ^{19}F NMR signals observed in the initial low-temperature spectra disappear when the solution is warmed. When the initial spectra are recorded at even lower temperatures, *e.g.* 215 K, both of these resonances have greater intensity than that of F_A, which implies that they may be due to intermediates in the formation of the acyl fluoride metal complex. Under high resolution, F_D is a triplet (coupling characteristic of $^2J_{PF}$) which is unaffected by proton decoupling and is related to a doublet at δ −10.2 in the ^{31}P-{^1H} NMR spectrum. These resonances are readily assigned to the monofluorinated cationic osmium(II) complex, **3a**; in particular, the unusually low-frequency ^{19}F NMR resonance (δ −421) compares very well with that obtained for the analogous cation $[OsF(CO)_5]^+$ (δ −433),[4] which can be rationalised in terms of the electron density at the metal centre. The ^{31}P NMR resonances for **2a** and **3a** show a corresponding low-frequency shift between the neutral and cationic complexes.

Under high resolution, F_E is a doublet of triplets which collapses to a triplet on proton decoupling (triplet coupling characteristic of $^2J_{PF}$). The related ^{31}P-{^1H} NMR resonance is a doublet. The ^{19}F chemical shift and the ^{31}P NMR spectrum indicate a monofluorinated neutral osmium(II) complex. A low-temperature ^1H NMR spectrum revealed that F_E is coupled to a doublet resonance at δ 10.7 ($^2J_{HF}$ = 46 Hz), confirming that the complex is monofluorinated. This resonance, which is typical of a metal-bound formyl (–COH),[11] allows assignment of this third low-temperature species to complex **4a**. The absence of coupling between the formyl proton and the triphenylphosphine ligands suggests that there may be some through-space interaction between F_E and the proton. The formation of this species cannot be explained by the reaction of a small quantity of HF with the osmium(0) or osmium(II)

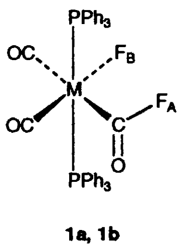

1a, 1b

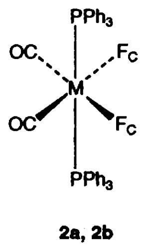

2a, 2b

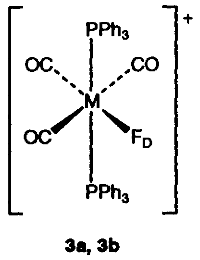

3a, 3b

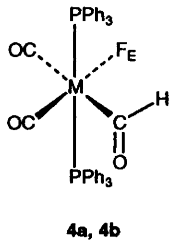

4a, 4b

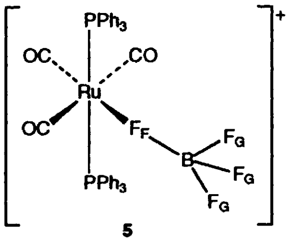

5

Table 1 NMR data for complexes **1–5**[a]

Complex	δ(^{31}P)[b]	δ(^{19}F)[b]		$^2J_{PF}$/Hz
1a $[OsF(COF)(CO)_2(PPh_3)_2]$	0.1 (d)	−370 (t)	F_B	30
		146 (s)	F_A	—
1b $[RuF(COF)(CO)_2(PPh_3)_2]$	19.6 (d)	−380 (t)	F_B	18
		156 (s)	F_A	—
2a $[OsF_2(CO)_2(PPh_3)_2]$[c]	1.4 (t)	−305 (t)	F_C	29
2b $[RuF_2(CO)_2(PPh_3)_2]$[c]	22.2 (t)	−318 (t)	F_C	19
3a $[OsF(CO)_3(PPh_3)_2]^+$	−10.2 (d)	−421 (t)	F_D	29
3b $[RuF(CO)_3(PPh_3)_2]^+$	not observed	−436 (t)	F_D	19
4a $[OsF(COH)(CO)_2(PPh_3)_2]$	0.4 (d)	−321 (d,t)[d]	F_E	25
4b $[RuF(COH)(CO)_2(PPh_3)_2]$	24.7 (d)	−316 (d,t)[e]	F_E	16
5 $[RuF(CO)_3(PPh_3)_2{\cdot}BF_3]^+$[f]	21.2 (d)	−302 (t,q)[g]	F_F	10
		−155 (d)[g]	F_G	—

[a] Spectra recorded at 220 K in CD_2Cl_2 solution unless otherwise noted. [b] Multiplicities in parentheses. [c] Recorded at 298 K. [d] Proton NMR resonance observed at δ 10.7; $^2J_{HF}$ = 46 Hz. [e] Proton NMR resonance observed at δ 10.1; $^2J_{FH}$ = 54 Hz. [f] Recorded at 215 K. [g] $^2J_{FF}$ = 88 Hz.

Table 2 Atomic coordinates (×10^4) for $[RuF_2(CO)_2(PPh_3)_2]\cdot CD_2Cl_2$

Atom	*x*	*y*	*z*
Ru	0	2748(1)	2500
P(1)	1022(1)	2783(2)	3548(1)
F(1)	508(2)	4139(4)	2069(2)
C(1)	511(3)	1556(7)	2088(3)
O(1)	806(3)	811(6)	1823(3)
C(11)	609(3)	2538(5)	4295(3)
C(12)	−3(4)	3293(8)	4384(3)
C(13)	−365(5)	3126(11)	4939(4)
C(14)	−112(6)	2168(11)	5397(5)
C(15)	522(7)	1435(9)	5308(5)
C(16)	863(4)	1600(7)	4768(4)
C(21)	1774(3)	1554(5)	3584(3)
C(22)	1524(4)	352(6)	3457(4)
C(23)	2070(4)	−591(7)	3456(4)
C(24)	2838(5)	−338(9)	3569(4)
C(25)	3110(4)	861(9)	3695(5)
C(26)	2575(4)	1815(7)	3693(4)
C(31)	1617(3)	4184(5)	3746(3)
C(32)	1857(4)	4803(8)	3225(4)
C(33)	2369(4)	5810(8)	3377(4)
C(34)	2636(4)	6203(7)	4013(5)
C(35)	2404(4)	5606(6)	4544(4)
C(36)	1882(4)	4590(6)	4404(3)
C(2)	5000	1676(16)	2500
Cl(1)	4308(3)	2665(4)	2792(2)

Table 3 Selected bond lengths (Å) and angles (°)

Ru–P(1)	2.406(1)	Ru–F(1)	2.011(4)
Ru–C(1)	1.841(7)	Ru–P(1A)	2.406(1)
Ru–F(1A)	2.011(4)	Ru–C(1A)	1.841(7)
P(1)–C(11)	1.804(7)	P(1)–C(21)	1.830(6)
P(1)–C(31)	1.805(6)	C(1)–O(1)	1.135(9)
P(1)–Ru–F(1)	93.6(1)	P(1)–Ru–C(1)	94.3(2)
F(1)–Ru–C(1)	91.7(2)	P(1)–Ru–P(1A)	178.2(1)
F(1)–Ru–P(1A)	85.1(1)	C(1)–Ru–P(1A)	86.9(2)
P(1)–Ru–F(1A)	85.1(1)	F(1)–Ru–F(1A)	84.4(2)
C(1)–Ru–F(1A)	176.0(2)	P(1A)–Ru–F(1A)	93.6(1)
P(1)–Ru–C(1A)	86.9(2)	F(1)–Ru–C(1A)	176.0(2)
C(1)–Ru–C(1A)	92.2(4)	P(1A)–Ru–C(1A)	94.3(2)
F(1A)–Ru–C(1A)	91.7(2)	Ru–P(1)–C(11)	112.0(2)
Ru–P(1)–C(21)	112.9(2)	C(11)–P(1)–C(21)	105.3(3)
Ru–P(1)–C(31)	117.8(2)	C(11)–P(1)–C(31)	104.1(3)
C(21)–P(1)–C(31)	103.5(3)	Ru–C(1)–O(1)	178.1(5)

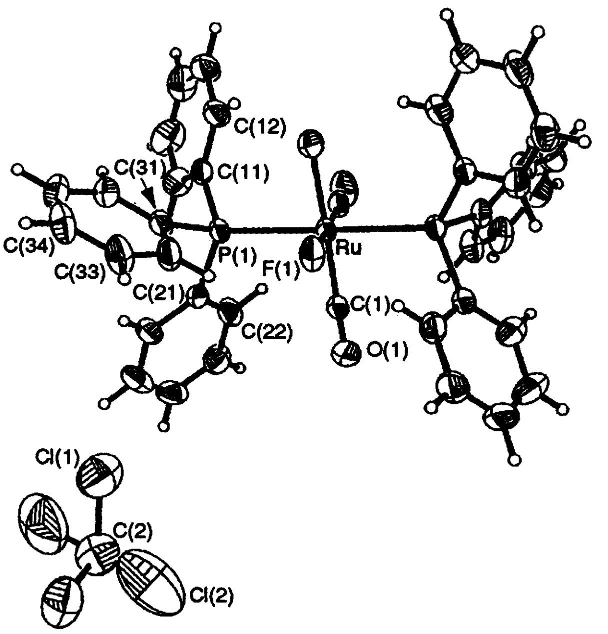

Fig. 1 Molecular structure of [*OC*-6-13]$[RuF_2(CO)_2(PPh_3)_2]$

complexes since **4a** is not observed in our investigations of the reaction of $[Os(CO)_3(PPh_3)_2]$ with HF, with and without XeF_2.[12] The most reasonable explanation, therefore, is that the species is formed by the reaction of HF with the cationic complex **3a**. The formation of **4a** is, therefore, a competing reaction with that resulting in the formation of **1a**.

The reaction of $[Ru(CO)_3(PPh_3)_2]$ with XeF_2 in CD_2Cl_2 was studied in an identical manner. Application of ^1H, ^{19}F and ^{31}P NMR spectroscopies revealed a directly analogous chemistry, with the formation of the ruthenium derivatives **1b**–**4b** (Table 1). The only significant difference between the two systems is the temperature of each particular transition. At 220 K, **3b** and **4b** were present, but **1b** was absent. On warming to 230 K, resonances due to **1b** started to appear while those due to **3b** decreased in intensity. Above 260 K all the resonances due to **1b**, **3b** and **4b** decreased in intensity and only the triplet resonances (^{19}F, δ −318; ^{31}P, δ 22.2; $^2J_{PF}$ = 19 Hz) assignable to [*OC*-6-13]$[RuF_2(CO)_2(PPh_3)_2]$ **2b** are present. Removal of the solvent affords an orange-brown solid which exhibits two IR-active ν(C–O) stretching vibrations at 2045 and 1973 cm^{-1} as expected. In the FAB mass spectrum the parent ion was not observed, but a series of patterns centred around *m*/*z* 701, 692, 682, 673, 654 and 626 are readily assigned to $[M - F]^+$, $[M - CO]^+$, $[M - 2F]^+$, $[M - F - CO]^+$, $[M - 2F - CO]^+$ and $[M - 2F - 2CO]^+$ respectively. The greater reactivity of the ruthenium(II) complexes over their osmium(II) analogues is completely in agreement with earlier work on the strength of the M–CO bond for these metals,[13] and our observations on the fluorination of $[Ru_3(CO)_{12}]$ and $[Os_3(CO)_{12}]$ with XeF_2.[3,4]

To date, our assignment of the [*OC*-6-13] ligand arrangement in these types of complex has relied entirely upon IR and NMR chemical shift and coupling-constant data. We are now able to support these assignments by a single-crystal structure determination of the final product from the ruthenium reaction. There have been relatively few single-crystal structure determinations of low-valent transition-metal fluoride complexes,[14] however crystals of [*OC*-6-13]$[RuF_2(CO)_2(PPh_3)_2]$ were obtained from a CD_2Cl_2 solution, by slow vapour diffusion with diethyl ether. X-Ray analysis has shown that the molecule is effectively octahedral with the predicted ligand arrangement (Fig. 1). The Ru–C, Ru–P and C–O bond lengths are comparable to those of related ruthenium(II) complexes.[15] The Ru–F bond length [2.011(4) Å], as expected, is significantly longer than the Ru–F (terminal) bond lengths determined by X-ray crystallography and extended X-ray absorption fine structure (EXAFS) for binary and ternary fluorides and fluoroanions of Ru^{IV}, Ru^{V} and Ru^{VI} (1.793–1.916 Å).[16–19] It is, however, very similar to the only other crystallographically characterised carbonylfluoride complexes of d^6 transition metals, $[ReF(CO)_3(Me_2NCH_2CH_2NMe_2)]$,[20] $[\{RuF_2(CO)_3\}_4]$,[3] $[IrF(COF)(CO)_2(PEt_3)_2][BF_4]$[1] and $[IrF(Cl)(NSF_2)(CO)(PPh_3)_2]$,[21] all of which contain fluoride *trans* to a carbonyl ligand, for which the M–F bond lengths fall in the range 2.089–1.998 Å.

The room-temperature stability of complex **1a** has allowed us to probe the mechanism of fluorination by its reaction with BF_3. In earlier studies on the oxidative fluorination of the isoelectronic iridium(I) species a mechanism involving two steps [equations (1) and (2)] was put forward. However, from the

$$[Ir(CO)_3(PEt_3)_2]^+ + XeF^+ \longrightarrow [IrF(CO)_3(PEt_3)_2]^{2+} + Xe \quad (1)$$

$$[IrF(CO)_3(PEt_3)_2]^+ + F^- \longrightarrow [IrF(COF)(CO)_2(PEt_3)_2]^+ \quad (2)$$

available evidence, it was not possible to differentiate between attack of F^- at the co-ordinated CO or migration of the metal-bound fluoride to CO and co-ordination of F^- at the iridium centre in step (2).

On warming a frozen solution of complex **1a** and BF_3 in CD_2Cl_2 reaction occurred below 215 K resulting in the formation of **3a** and BF_4^-. Hence, fluoride abstraction by BF_3 appears to occur preferentially at the acyl fluoride. This preference for abstraction, by BF_3, of fluoride from a co-ordinated fluorinated ligand over a metal-bound fluoride has been noted previously,[22] in the reaction of $[IrF(Cl)(CO)(SF_3)(PEt_3)_2]$ with BF_3. Furthermore, since the Os–F bond in **3a** does not undergo further reaction with an excess of BF_3, even at room temperature, these results substantiate the proposed mechanism involving nucleophilic attack by F^- at co-ordinated CO.

Similar results are obtained in the reaction of complex **1b** with BF_3 where **3b** and BF_4^- are readily identified in the ^{19}F NMR spectra. For this system, however, low-temperature (215 K) ^{19}F and ^{31}P NMR spectra reveal the formation of a thermally unstable BF_3 adduct **5**. The RuF resonance (δ −302.3) for this species is a triplet of quartets. The triplet splitting ($^2J_{PF}$ = 10 Hz) is due to coupling to *trans*-phosphine ligands which appear as a doublet at δ 21.2 in the ^{31}P NMR spectrum. The quartet splitting ($^2J_{FF}$ = 88 Hz) is due to coupling to fluorine on the adduct BF_3 which appears as a doublet at δ −155. Co-ordination of BF_4^- to metal centres has been observed previously. For species of the type $[M(C_5H_5)(CO)_2L][BF_4]$ [M = Mo or W; L = CO, PPh_3 or $P(OPh)_3$] the co-ordinated and terminal fluorine atoms of the BF_4^- ligand can also be distinguished by their low-temperature ^{19}F NMR signals.[23] These results suggest that the M–F bond for M = Ru is more strongly polarisable than that for M = Os.

Conclusion

The stepwise oxidative addition of xenon difluoride to ruthenium(0) and osmium(0) reagents occurs readily at low temperatures; the mechanium involves oxidation by XeF^+, nucleophilic attack by F^- at co-ordinated CO followed ultimately by elimination of CO to yield stable, octahedral, $[MF_2(CO)_2(PPh_3)_2]$. These results give further support to the assertion that the fluoride ligand and low-valent transition metals are not mutually incompatible. All of the products and intermediates have been characterised by multinuclear NMR spectroscopy in solution, in particular extending the characteristic metal-bound fluoride ^{19}F NMR chemical shift data to new metals and new ligand environments.

Acknowledgements

We thank the SERC (S. A. B., K. S. C. and E. G. H.) and ICI Klea Group (P. G. W.) for financial support. We also acknowledge the preliminary results obtained for the ruthenium system by P. G. W. whilst working with Professor E. A. V. Ebsworth at the University of Edinburgh.

References

1 A. J. Blake, R. W. Cockman, E. A. V. Ebsworth and J. H. Holloway, *J. Chem. Soc., Chem. Commun.*, 1988, 529.
2 E. A. V. Ebsworth, N. Robertson and L. J. Yellowlees, *J. Chem. Soc., Dalton Trans.*, 1993, 1031.
3 C. J. Marshall, R. D. Peacock, D. R. Russell and I. L. Wilson, *Chem. Commun.*, 1970, 1643.
4 S. A. Brewer, J. H. Holloway and E. G. Hope, *J. Chem. Soc., Dalton Trans.*, 1994, 1067.
5 J. H. Holloway, *Chem. Commun.*, 1966, 22.
6 N. Ahmad, J. J. Levison, S. D. Robinson and M. F. Uttley, *Inorg. Synth.*, 1974, **15**, 45.
7 K. R. Grundy, *Inorg. Chim. Acta*, 1981, **53**, L225.
8 W. W. Dukat, J. H. Holloway, E. G. Hope, P. J. Townson and R. L. Powell, *J. Fluorine Chem.*, 1993, **62**, 293.
9 G. M. Sheldrick, SHELXTL-PC, Release 4.1, Program for crystal structure determination and refinement, Siemens Analytical X-Ray Instruments, Madison, WI, 1990.
10 R. W. Cockman, E. A. V. Ebsworth, J. H. Holloway, H. Murdoch, N. Robertson and P. G. Watson, *ACS Symp. Ser.*, 1994, **555**, 326.
11 G. R. Clark, C. E. L. Headford, K. Marsden and W. R. Roper, *J. Am. Chem. Soc.*, 1979, **101**, 503; W. Tam, W.-K. Wong and J. A. Gladysz, *J. Am. Chem. Soc.*, 1979, **101**, 1589.
12 S. A. Brewer, L. A. Buggey, J. H. Holloway and E. G. Hope, unpublished work.
13 G. Cetini, O. Gambino, E. Sappa and G. A. Vaglio, *Atti Accad. Sci. Torino*, 1966, **101**, 1.
14 N. M. Doherty and N. W. Hoffman, *Chem. Rev.*, 1991, **91**, 573.
15 A. G. Orpen, L. Brammer, F. H. Allen, O. Kennard, D. G. Watson and R. Taylor, *J. Chem. Soc., Dalton Trans.*, 1989, S1.
16 M. A. Hepworth, K. H. Jack, R. D. Peacock and G. J. Westland, *Acta Crystallogr.*, 1957, **10**, 63.
17 N. Bartlett, H. Borrmann and W. J. Casteel, jun., *Inorg. Chem.*, 1992, **31**, 3124.
18 J. W. Cable, H. R. Child, M. K. Wilkinson and E. O. Wollan, *Phys. Rev.*, 1961, **121**, 74.
19 A. K. Brisdon, J. H. Holloway, E. G. Hope, W. Levason, J. S. Ogden and A. K. Saad, *J. Chem. Soc., Dalton Trans.*, 1992, 447.
20 E. Horn and M. R. Snow, *Aust. J. Chem.*, 1984, **37**, 35.
21 P. G. Watson, E. Lork and R. Mews, *J. Chem. Soc., Chem. Commun.*, 1994, 1069.
22 R. W. Cockman, E. A. V. Ebsworth and J. H. Holloway, *J. Am. Chem. Soc.*, 1987, **109**, 2194.
23 K. Sunkel, G. Urban and W. Beck, *J. Organomet. Chem.*, 1983, **252**, 187.

Received 11*th November* 1994; *Paper* 4/06886F